PHYSICAL REVIEW B VOLUME 52, NUMBER 7 15 AUGUST 1995-I

ARTICLES

Reflectance of conducting polypyrrole: Observation of the metal-insulator transition driven by disorder

Kwanghee Lee, Reghu Menon, C. O. Yoon, and A. J. Heeger
Institute for Polymers and Organic Solids, University of California at Santa Barbara, Santa Barbara, California 93106
(Received 3 January 1995; revised manuscript received 1 May 1995)

By controlling the extent of disorder through electrochemical synthesis at reduced temperatures, conducting polypyrrole (PPy) can be obtained in the metallic regime, in the insulating regime, and in the critical regime of the disorder-induced metal-insulator (*M-I*) transition. We present the results of reflectance measurements (0.002–6 eV) of PPy carried out at room temperature on the metallic side and on the insulating side of the *M-I* transition. While the reflectance spectra obtained from samples on both sides of the *M-I* transition exhibit spectral features expected for a partially filled conduction band, the electronic states near the Fermi energy (E_F) are different in the two regimes. The data obtained from metallic samples indicate delocalized electronic wave functions in the conduction band, whereas the spectral features which characterize the insulating regime indicate that the states near E_F are localized. Consistent with theoretical predictions for the metallic and insulating regimes, the optical conductivity $\sigma(\omega)$ and the real part of the dielectric function $\varepsilon_1(\omega)$ each show different frequency dependences in the far infrared. In the metallic regime $\sigma(\omega) \propto \omega^{1/2}$ for $\hbar\omega < 600\ \mathrm{cm}^{-1}$ and $\varepsilon_1(\omega)$ (>0) increases rapidly as $\omega \rightarrow 0$, as described by the "localization-modified Drude model," leading to the conclusion that metallic polypyrrole is a *disordered metal* near the *M-I* transition. In contrast, the insulating regime is characterized as a *Fermi glass* as confirmed by $\sigma(\omega) \propto \omega^2$ for $\hbar\omega < 600\ \mathrm{cm}^{-1}$.

I. INTRODUCTION

The dynamics of single-particle excitations in the partially filled conduction band of crystalline metals are governed by coherent diffusion processes; electrons drift ballistically and make random collisions with defects and with phonons, resulting in finite resistivity. The classical treatment of the contribution to the complex dielectric function, $\varepsilon(\omega)=\varepsilon_1(\omega)+i(4\pi/\omega)\sigma(\omega)$, associated with the low-energy (intraband) excitations in terms of the free-electron approximation (the Drude model) has been broadly successful in describing the electronic properties of simple metals.[1] When disorder is introduced, with the magnitude of disorder potential comparable to the bandwidth, multiple scattering causes the electronic states near the Fermi energy (E_F) to become localized.[2,3] Even though there is a finite density of states at E_F in such a system, disorder-induced localization causes a transition from metal to insulator. As a result, the charge dynamics of disordered systems are expected to be fundamentally different from those which characterize traditional metallic behavior.[2–4]

The electronic states of conducting polymers are strongly influenced by disorder.[5,6] Although heavily doped conducting polymers have a metallic density of states at E_F, their transport properties are dominated by the disorder which originates from a combination of partial crystallinity (molecular scale disorder) and/or inhomogeneous doping.[5–8] Recent progress in the synthesis and processing of conducting polymers has significantly reduced the structural disorder.[9–11] These structurally improved materials provide opportunities for studying the metal-insulator (*M-I*) transition by controlling the extent of disorder.[12,13]

The question of whether the disorder is present on a molecular scale or whether the properties are dominated by more macroscopic inhomogeneities (metallic islands) has been a subject of considerable discussion. Examples of materials with macroscopic inhomogeneity exist in the literature.[14] In the case of polyaniline, when processed from solution in the conducting form (for example, protonated with camphor sulfonic acid, PANI-CSA, and processed from *m*-cresol), the material is more homogeneous with disorder on many length scales. Although the wide-angle x-ray-diffraction patterns of PANI-CSA exhibit both crystalline and amorphous features, the coherence length of the crystalline regions is less than either the localization length or the inelastic-scattering length.[15] Consequently, the transport data obtained from PANI-CSA have been analyzed in terms of a disordered metal close to the metal-insulator transition.[15,16]

Polyaniline blends[16] are particularly interesting in this context, for electron microscopy studies have demonstrated that these can cross over from a homogeneous system with interconnected structure to an inhomogeneous system with metallic islands on going below the percolation threshold. Below the percolation threshold, the transport follows the behavior expected of granular met-

als,[17] $\ln\sigma(T) \propto -(T_0/T)^{1/2}$. In pure PANI-CSA, however, $\ln\sigma(T) \propto -(T_0/T)^{1/4}$, characteristic of variable range hopping between microscopically localized states in three dimensions.[15]

When electrochemically synthesized at low temperatures under rigorous conditions, polypyrrole (PPy) doped with PF_6, hereafter simply denoted as PPy(PF_6), exhibits improved transport properties, achieving a higher dc conductivity at room temperature, $\sigma_{dc}(300\ \mathrm{K}) \approx 200-500$ S/cm and a weaker temperature dependence of σ_{dc} than observed previously in doped polypyrrole.[9,10] Recent transport studies[13] on this system were successful in characterizing the extent of disorder in terms of the temperature dependence of the resistivity $\rho(T)$, more specifically the resistivity ratio $\rho_r \equiv \rho(1.4\ \mathrm{K})/\rho(300\ \mathrm{K})$. For $\rho_r < 10$, the system is metallic, with $\rho(T)$ remaining finite as $T \to 0$, whereas for $\rho_r > 10$, the system is an insulator with $\rho_r \to \infty$ as $T \to 0$.[13] Thus PPy(PF_6) undergoes a M-I transition at $\rho_r \approx 10$. The correlation length (L_c), inferred from the extrapolated $\sigma_{dc}(T \to 0)$ in the metallic regime and from the analysis of the magnetoresistance in the insulating regime, diverges as the M-I transition is approached from either side,[13] as expected from both theory[2,3] and experiment.[18]

Although comprehensive studies[13] of the transport properties provide unambiguous evidence of the disorder-induced M-I transition in PPy(PF_6), implying a change in the nature of the states at E_F from localized states to extended states, much less is known about the differences in charge dynamics in the metallic and insulating regimes. Therefore, optical spectra for materials on both sides of the M-I transition must be examined and compared in order to probe the nature of the electronic states near the E_F and to investigate the role of disorder in the electronic structure.

Reflectance measurements provide information on the electronic structure and on the nature of low-lying elementary excitations over a wide energy range.[19] In particular, measurements in the infrared (IR) spectral range probe the charge dynamics involving intraband excitations; i.e., excitations within the partially filled conduction band. In this work, we reported the reflectance spectra of PPy(PF_6) in the metallic and insulating regimes over a wide spectral range (0.002–6 eV). The reflectance spectra of both regimes exhibit spectral features expected for a partially filled conduction band with a similar band structure. However, detailed analyses of the spectra clearly bring out the different nature of the electronic states near E_F. In the metallic regime, the electronic states in the conduction band are modestly delocalized ($k_F l > 1$, where k_F is the Fermi wave number and l is the mean free path), whereas the data from the insulating regime indicate localized states near E_F. Improvements in sample quality induce the transition from insulator to metal, implying a crossover in the relative positions of E_F and the mobility edge (E_C). Studies of metallic samples, therefore, allow a quantitative analysis of the charge dynamics involving intraband excitations (within the conduction band), reflecting the intrinsic metallic properties of the PPy(PF_6).

II. EXPERIMENT

A. Sample preparation and characterization

Free-standing films of PPy(PF_6) were prepared by electrochemical polymerization as described in detail in earlier publications.[9,13] Pyrrole was polymerized and doped by anodic oxidation in an electrochemical cell. A glassy carbon electrode and platinum foil were used for the working and counter electrode, respectively. A constant current (0.1–0.3 mA/cm^2) was applied under a nitrogen atmosphere. Different polymerization conditions were used to synthesize the metallic (M) and insulating (I) samples. For M samples, the polymerization temperature was maintained at $-40\,^{\circ}\mathrm{C}$, whereas I samples were prepared at room temperature. Other sample preparation conditions are more or less identical for the two cases as described in detail elsewhere.[13] Lustrous dark free-standing films were peeled off the electrode, then dried under vacuum for 24 h. The surface quality of these films was sufficient for the reflectance measurements without concern for scattering losses. Film thicknesses were typically 10–15 μm.

Detailed characterization of PPy(PF_6) synthesized under conditions used for preparing the films for the IR measurements have been carried out by Yamaura *et al.*[20] and Hagiwara *et al.*,[21] including, for example, infrared spectra, x-ray diffraction, scanning electron microscopy, etc. As is typical of conducting polymers, the x-ray-diffraction patterns show crystalline and amorphous regions. In PPy(PF_6), however, the coherence length of the crystalline regions is only approximately 20 Å,[22] much less then either the localization length or the inelastic-scattering length.[13] Consequently, the transport data obtained from PPy(PF_6) have been successfully analyzed in terms of a disordered metal close to the metal-insulator boundary.[13]

Several samples were prepared in each sample category (metallic regime, critical regime, and insulating regime). Although the sample preparation conditions are nearly identical within the same sample category, the extent of disorder is influenced by details of the synthesis and processing.[13] Such subtle changes in morphology and crystallinity lead to corresponding changes in the electrical properties.[13] These changes in electrical properties have been fully described. A conclusion of these studies was that the disorder can be characterized uniquely in terms of the resistivity ratio.[13] The corresponding resistivity ratios for the samples utilized in this infrared reflectance study are summarized below.

We have found that the reflectance spectra within the same sample category (i.e., the metallic side of the metal-insulator transition versus the insulator side of the metal-insulator transition) were insensitive to such subtle differences in transport behavior. The reflectance spectra for each category of samples were quite general with excellent reproducibility.

The transport properties of all films were measured in order to fully characterize the samples and to assure the sample quality. Figure 1 shows the temperature dependence of the resistivity $\rho(T)$ normalized by $\rho(300\ \mathrm{K})$ for

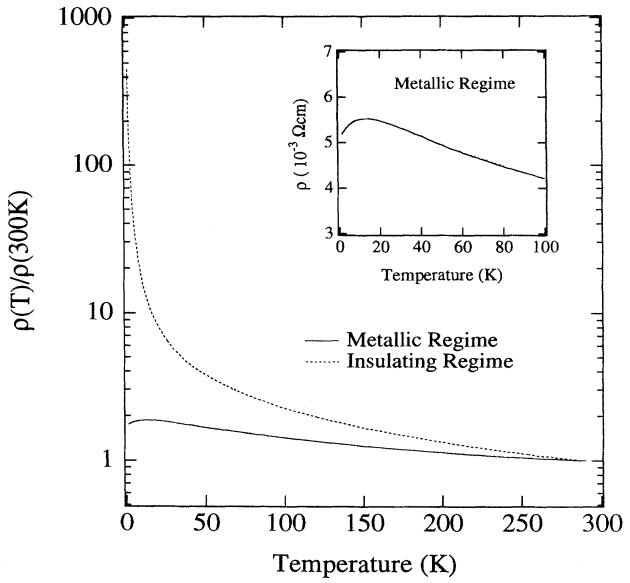

FIG. 1. Temperature dependence of the resistivity, $\rho(T)$, of $PPy(PF_6)$, normalized by $\rho(300\ K)$ for samples in the metallic regime (M) and in the insulating regime (I). The inset shows the resistivity maximum for the metallic regime sample at low temperature.

the M and I samples. As noted above, $\rho(T)$ is sensitive to the polymerization conditions, demonstrating an obvious contrast between M and I, especially at low temperatures. Based on the transport measurements,[13] sample M corresponds to the metallic regime ($\rho_r = 1.75 < 10$), whereas sample I is in the insulating regime ($\rho_r = 453 > 10$). As reported in previous studies,[9,10,13] a resistivity maximum is observed for sample M around 13 K, below which the resistivity shows a positive temperature dependence ($d\rho/dT > 0$). For sample M, $\sigma_{dc}(300\ K) \approx 340$ S/cm, while sample I shows $\sigma_{dc}(300\ K) \approx 50$ S/cm.

B. Optical measurements

Reflectance was measured between 20 and 50 000 cm^{-1} (0.002–6 eV) using three different spectrometers. IR reflectance in the range of 50–9000 cm^{-1} was measured with a Nicolet Magna-750 Fourier Transform Interferometer (FTIR). For the longest wavelengths (20–100 cm^{-1}), a Bomem DA3.002 FTIR equipped with a ^{3}He-cooled Si bolometer (operated at 300 mK) was used. Excellent agreement was obtained for data from the two different instruments in the region of overlap. Visible UV range spectra were obtained using a Perkin-Elmer λ-9 grating monochrometer. Again, the agreement of the spectra between overlap spectral regions with different instruments was excellent. A gold mirror was used as a reference in the IR, and an aluminum mirror was used in the visible UV range. The data were corrected using the reflectance spectra of the references as given in the literature.[19,23]

The optical conductivity $\sigma(\omega)$ and dielectric function $\varepsilon(\omega)$ were obtained by Kramers-Kronig (KK) analysis of the reflectance spectra. Since KK transformation requires a knowledge of the reflectance over the full spectral range ($0 < \hbar\omega < \infty$), reasonable and careful extrapolations were made to lower and higher energies (i.e., beyond the measurement range).[19] At energies between 6 eV and E_{fg}(25 eV $\leq E_{fg} \leq$ 50 eV), the reflectance spectra were extrapolated as ω^{-s}, where $1 \leq s \leq 4$. Above E_{fg}, the data were extrapolated according to the asymptotic behavior of free electrons ($\propto \omega^{-4}$), as described in the literature.[19] In this procedure, the terminating energy E_{fg} and exponent s were determined so as to give consistent optical spectra over a wide range. Since we are concerned with the low-energy region for establishing the details of the metal physics, the extrapolation to the higher region has little effect on the results. At lower frequencies ($\hbar\omega < 0.01$ eV), the reflectance spectra were extrapolated by the Hagen-Rubens relation.

III. RESULTS AND DISCUSSION

A. Reflectance, $R(\omega)$

Figure 2 shows the reflectance (R) of $PPy(PF_6)$ for samples in the metallic regime and for samples in the insulating regime, measured at room temperature. Both spectra exhibit a reflectance minimum, around 1.8 eV for the metallic regime and 2 eV for the insulating regime, indicative of a plasma resonance due to free carriers in the conduction band. Below the minimum, R increases with decreasing frequency, with a rapid rise below 0.2 eV as $\omega \to 0$. For the metallic regime, R reaches almost 85% in the far-IR ($\omega \leq 100\ cm^{-1}$). The high reflectance in the far-IR and the free-carrier plasma resonance are traditional signatures of metallic behavior.[19,23,24] For the insulating regime, R also increases with decreasing frequency for $\hbar\omega < 2$ eV, but $R(\omega)$ remains well below that of the

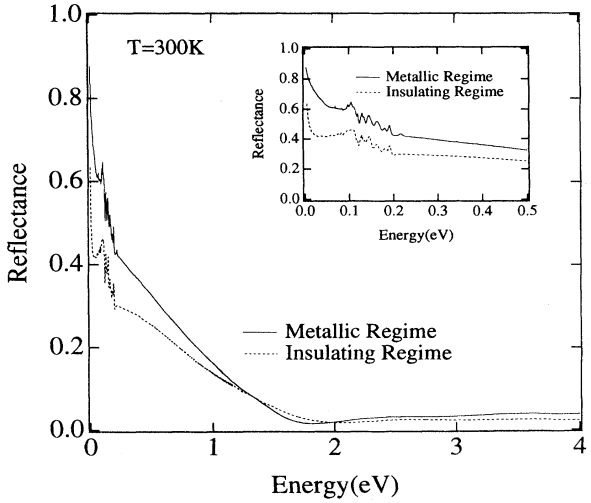

FIG. 2. Reflectance spectra of $PPy(PF_6)$ in the metallic regime (solid line) and in the insulating regime (dotted line) measured at room temperature. The inset shows the low-energy spectra ($\hbar\omega < 0.5$ eV) with an expanded scale.

metallic regime throughout the IR ($\hbar\omega < 1$ eV). Obvious phonon features appear around 0.1–0.2 eV for both regimes.

B. Optical conductivity, $\sigma(\omega)$

Figure 3 shows the optical conductivity $\sigma(\omega) = \omega\varepsilon_2(\omega)/4\pi$ for $\hbar\omega < 4$ eV. As expected from the characteristic metallic features in $R(\omega)$ for both regimes, $\sigma(\omega)$ is dominated by intraband excitations (within the conduction band) for $\hbar\omega < 2$ eV; and interband transitions are observed at 2.7 and 3.7 eV. The similarity in the spectral features for samples from the two regimes indicates their common electronic band structure.

In spite of the characteristic metallic signatures in the reflectance spectra, however, the corresponding $\sigma(\omega)$ are not typical of a good metal. Even for the metallic regime, $\sigma(\omega)$ deviates considerably from the normal Drude behavior below 0.4 eV; in contrast to Drude behavior, $\sigma(\omega)$ is suppressed as $\omega \to 0$. This decrease in $\sigma(\omega)$ arises from weak localization, as demonstrated in previous work on polyaniline doped with camphor sulfonic acid (PANI-CSA).[24] For the insulating regime, however, $\sigma(\omega)$ is suppressed even more at low frequencies, indicating that the states near E_F in the conduction band are localized. The localization arises from disorder in the context of Anderson localization.[2,3] Indeed, in early spectroscopic studies on the heavily doped conducting polymers, such a suppressed $\sigma(\omega)$ was observed and interpreted as a pseudogap feature.[25,26] However, an interpretation in terms of localization of the intraband excitations in highly disordered materials is more reasonable and consistent with all the facts.

The effects of strong disorder can be seen in the interband transitions as well as in the intraband excitations.

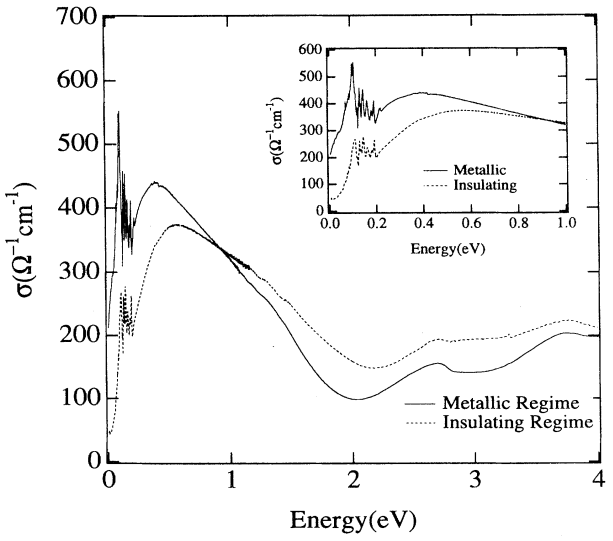

FIG. 3. Optical conductivity, $\sigma(\omega)$, of $PPy(PF_6)$ in the metallic regime (sold line) and in the insulating regime (dotted line), obtained from KK analysis of the reflectivity data. The inset shows the spectra in the IR ($\hbar\omega < 1$ eV) with an expanded scale.

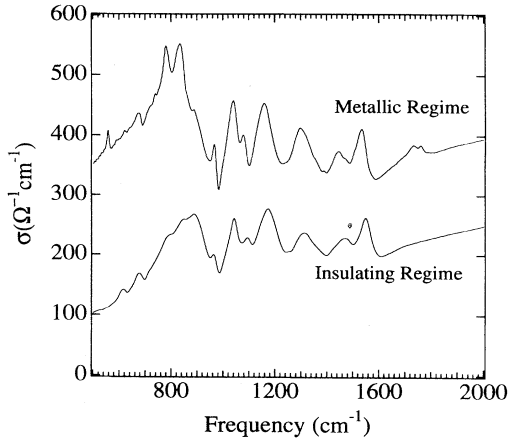

FIG. 4. Comparison of the phonon features shown in $\sigma(\omega)$ of $PPy(PF_6)$ in the metallic regime (solid line) and in the insulating regime (dotted line). Note the relatively featureless peak shape for the insulating regime, especially between 600 and 1000 cm^{-1}.

For example, in the insulating regime, the 2.7-eV feature is relatively weak peak in contrast to the sharp peak observed in the metallic regime. Disorder smears out the joint density of states by introducing states (and absorption) within the gap, resulting in broadening of the corresponding spectral features.[27,28] Furthermore, in such disordered systems, the wave vector is not a good quantum number.[3,29] As a result, lack of **k** conservation enables indirect transitions (otherwise forbidden), smearing out the joint density of states for the direct transitions (allowed). Lack of **k** conservation also results in suppression of the phonon features by allowing the interaction of light with all phonons, not only with IR-active modes. The relatively broad phonon features in the insulating regime (especially between the 600 and 1000 cm^{-1}) are compared with the sharp phonon features in the metallic regime in Fig. 4.

C. Dielectric function, $\varepsilon(\omega)$, and energy-loss function, $\mathrm{Im}[-1/\varepsilon(\omega)]$

Figure 5 shows the real part of dielectric function, $\varepsilon_1(\omega)$, for both regimes. Consistent with $\sigma(\omega)$, $\varepsilon_1(\omega)$ for the metallic regime does not follow the behavior expected of a pure Drude metal. Instead, $\varepsilon_1(\omega)$ remains positive over the entire spectral range below the plasma frequency (ω_p), and increases to larger positive values as $\omega \to 0$. This non-Durde behavior is again associated with disorder-induced localization.[24] For the insulating regime, $\varepsilon_1(\omega)$ exhibits large positive values below 0.8 eV, indicative of localization of the states near E_F. Note, however, the rapid increase of ε_1 for the metallic regime as $\omega \to 0$, with even higher values than for the insulating regime below 0.1 eV.

For a good metal with $\omega_p\tau > 1$ (where τ is the momentum relaxation time), $\varepsilon_1(\omega)$ is expected to cross zero at the screened plasma frequency, $\Omega_p = \omega_p/(\varepsilon_\infty)^{1/2}$, where

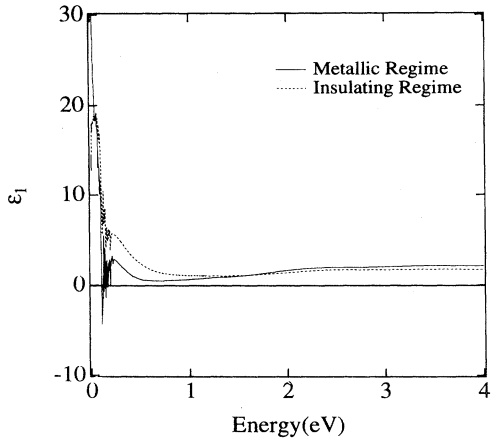

FIG. 5. Real part of the dielectric function, $\varepsilon_1(\omega)$, of $PPy(PF_6)$ in the metallic regime (solid line) and in the insulating regime (dotted line).

ε_∞ is the high-energy contribution to the dielectric constant. At low frequencies, $\varepsilon_1(\omega) \propto -(\omega_p/\omega)^2$ for $\omega > 1/\tau$ and $\varepsilon_1(\omega) \approx -(\omega_p \tau)^2$ for $\omega < 1/\tau$.[19,29] However, in dirty metals with $\omega_p \tau \sim 1$, the plasma oscillation is overdamped, preventing even the zero crossing at Ω_p. As a result, $\varepsilon_1(\omega)$ remains positive at all frequencies. This is the case for $PPy(PF_6)$.

The damping of the plasma resonance is evident in the spectral shape of the energy-loss function, $\mathrm{Im}[-1/\varepsilon(\omega)]$, as shown in Fig. 6. In the metallic regime, $\mathrm{Im}[-1/\varepsilon(\omega]$ exhibits a well-defined peak with a maximum at 1.4 eV with full width at half maximum (FWHM) of approximately 1 eV, corresponding to $\omega_p \tau \approx 1$. For the insulating regime, the FWHM is even larger, consistent with an overdamped plasma oscillating.

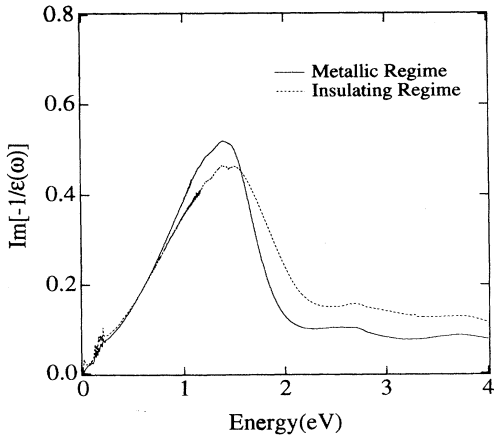

FIG. 6. Energy-loss function $\mathrm{Im}[-1/\varepsilon(\omega)]$ of $PPy(PF_6)$ in the metallic regime (solid line) and in the insulating regime (dotted line).

D. Effective number of carriers, $N_{\mathrm{eff}}(\omega)$

The integrated spectral weight provides information on the number of carriers contributing to the intraband excitations within the conduction band:

$$N_{\mathrm{eff}}(\omega) = \frac{2m^* V_{\mathrm{cell}}}{\pi e^2} \int_0^{\omega} \sigma(\omega') d\omega' , \tag{1}$$

where $N_{\mathrm{eff}}(\omega)$ is the effective number of carriers per unit cell contributing to $\sigma(\omega)$ at frequencies below ω, m^* is the effective mass of the electrons, and V_{cell} is the unit-cell volume. In calculating $N_{\mathrm{eff}}(\omega)$, we have used the approximate unit-cell dimensions[22] $a = 11.8$ Å, $b = 6.56$ Å, and $c = 3.4$ Å. The effective mass was assumed to be the free-electron masses m_e.

Figure 7 illustrates $N_{\mathrm{eff}}(\omega)$ for both regimes as calculated by Eq. (1); $N_{\mathrm{eff}}(\omega)$ shows similar behavior for both regimes. The only difference is observed at low energies due to the severe suppression of $\sigma(\omega)$ for the insulating regime. $N_{\mathrm{eff}}(\omega)$ increases smoothly up to $\hbar\omega = 2$ eV, and shows a slight saturation for $2.0\ \mathrm{eV} < \hbar\omega < 2.5$ eV consistent with exhausting the intraband oscillator strength. $N_{\mathrm{eff}}(\omega)$ increases again at higher energies due to the onset of the interband transitions. Since the oscillator strength associated with the intraband excitations is fully contained below 2.5 eV, $N_{\mathrm{eff}} \approx 0.6(m^*/m_e)$ at 2.5 eV provides an estimate of the effective number of carriers per unit cell involved in intraband excitations within the condition band. The x-ray structure analysis[22] indicates one free carrier per unit cell (i.e., one dopant per four pyrrole units), such that $N_{\mathrm{eff}} = 1$ per unit cell. Therefore, we conclude that the optimal mass (the effective mass averaged over the occupied states) is $m^* \approx 1.7 m_e$.

The two curves cross at about 3 eV. Note that $N_{\mathrm{eff}}(\omega)$ reflects the total number of carriers contributing to the oscillator strength up to frequency ω, regardless of whether they are itinerant or localized. Therefore, the

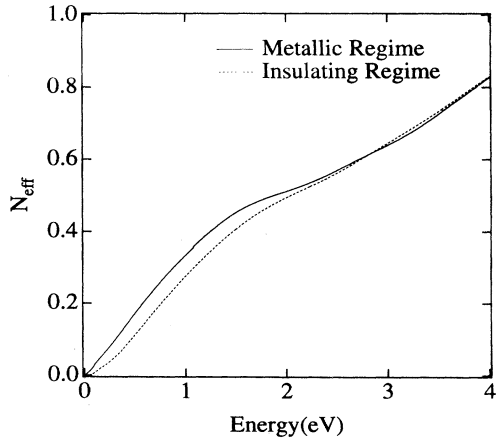

FIG. 7. The effective number of carriers per unit cell, $N_{\mathrm{eff}}(\omega)$, as a function of energy for $PPy(PF_6)$ in the metallic regime (solid line) and in the insulating regime (dotted line) obtained with Eq. (1). The effective mass was assumed to be that of the free electron.

crossover of $N_{\text{eff}}(\omega)$ at 3 eV implies that both regimes have an approximately equivalent total number of charge carriers involved in the intraband excitations.

E. *M-I* transition driven by disorder: Anderson localization

One might have assigned the different behavior of the *M* and *I* samples to differences in the doping level as obtained by the different polymerization conditions. However, the conservation of the oscillator strength of the intraband excitations shown in Fig. 7 implies almost identical densities of charge carriers, consistent with the Pauli spin susceptibility measurements.[30] Thus differences in charge-carrier density are not responsible for differences in optical features in the two regimes.

As illustrated by the transport measurements,[13] the principal difference between the *M* and *I* regimes originates from the degree of disorder. For the insulating regime, the disorder is sufficiently strong that the electronic states at E_F are localized in the context of Anderson localization. Thus, the insulating regime of PPy(PF_6) can be categorized as a *Fermi glass,* in which E_F lies in the region of localized states below the mobility edge (E_C). According to localization theory,[2,4,31,32] for the *Fermi glass* at low frequencies $\sigma(\omega)$ can be expressed as

$$\sigma(\omega)=\sigma(0)+b\omega^s , \tag{2}$$

where b and s are constants. For the value of the exponent s, both Mott's localization theory[2] and the scaling theory[4] of localization predict $\sigma(\omega)\propto\omega^2(s=2)$ for $\omega<\omega_c$, while $\sigma(\omega)\propto\omega^{1/3}$ ($s=\frac{1}{3}$) for $\omega>\omega_c$, where ω_c is the crossover frequency below which the effect of localization is substantial. Above this frequency, localization does not affect the carrier mobility due to photon-activated hopping between the localized states, so that high-frequency behavior is essentially metallic ($s<1$).[31] In Fig. 8, we have plotted $\sigma(\omega)$ for the insulating regime in the spectral range $\omega<4000$ cm^{-1} (0.5 eV), together with the theoretical fits. For $\omega<600$ cm^{-1}, the data are well described by the ω^2 dependence with $\sigma(0)=30$ S/cm and $b=2.2\times10^{-4}$, while, for $\omega>600$ cm^{-1}, $\sigma(\omega)\propto\omega^{1/3}$, in good agreement with theoretical predictions.[2,4,31–34] In spite of the overlap with the sharp phonon contributions, one can observe the crossover of the ω dependence in the IR with $\omega_c\approx600$ cm^{-1}. In doped semiconductors, however, ω_c appears in the microwave region.[31–34] The appearance of ω_c in the IR might be associated with the fact that the *M-I* transition in the conducting polymers occurs at much higher carrier concentrations ($n_c\approx10^{20-21}$) than in doped semiconductors ($n_c\approx10^{18-19}$). As a result, the energy scale ($\hbar\omega_c\approx n_c^{1/2}$) below which the effect of localization is significant is enhanced by one or two orders of magnitude in conducting polymers compared with doped semiconductors.

When the samples are prepared electrochemically at low temperature (−40 °C; i.e., in the metallic regime), there is a significant reduction in the extent of disorder. The reduced disorder changes in the relative position of E_C and E_F and delocalizes the electronic states near E_F.[2,3] However, the deviation of $\sigma(\omega)$ and $\varepsilon_1(\omega)$ from

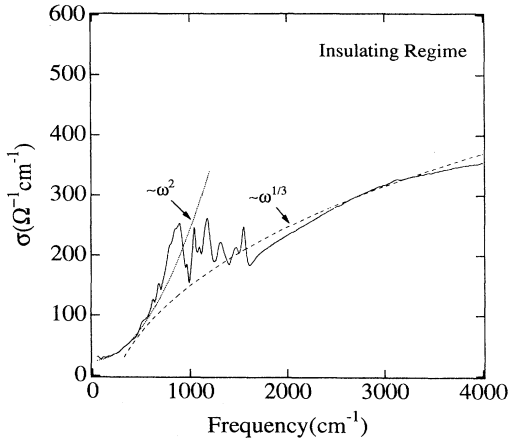

FIG. 8. Comparison of the measured $\sigma(\omega)$ (solid line) of PPy(PF_6) in the insulating regime with the theoretical prediction (dashed and dotted lines) given by Eq. (2). At low frequencies (below 600 cm^{-1}) the data were fit to $\sigma(\omega)\propto\omega^2$, while the high-frequency part (above 600 cm^{-1}) was approximated with a $\omega^{1/3}$ dependence.

the classical Drude behavior at low frequencies indicates that the electronic states are, nevertheless, influenced by the disorder. This observation implies that, in the metallic regime, PPy(PF_6) can be characterized as a *disordered metal* near the *M-I* boundary. In such a system, $\sigma(\omega)$ can be quantitatively analyzed in terms of the localization-modified Drude model

$$\sigma_{\text{LD}}(\omega)=\sigma_{\text{Drude}}\left[1-\frac{C}{(k_F l)^2}\left[1-\frac{l}{L_\omega}\right]\right] , \tag{3}$$

as confirmed in the analysis of polyaniline doped by camphor sulfonic acid (PANI-CSA).[24] The localization-modified Drude model includes the first-order correction term to $\sigma_{\text{Drude}}(\omega)=(\omega_p^2\tau/4\pi)[1+\omega^2\tau^2]^{-1}$ due to weak localization.[34] In the correction term, l is the mean free path ($l=v_F\tau$), k_F is the Fermi wave number, and L_ω is the distance scale over which an electron diffuses within the period of the incident radiation field. The constant C is of order unity. With the diffusion coefficient given by $D=l^2/3\tau$, L_ω can be expressed as $L_\omega=(D/\omega)^{1/2}$. Figure 9 illustrates the excellent agreement of theoretical expression with the data from the metallic regime with the following parameters: $\omega_p=14\,200$ cm^{-1} (1.8 eV), $1/\tau=9600$ cm^{-1} (1.2 eV), and $k_F l=1.6$. This value for $k_F l$ is the same as that obtained independently from analysis of the resistivity data.[13]

As expected from the theory,[31–34] the effect of localization is dominant only at low frequencies (below $\omega_c\approx600$ cm^{-1}). The different ω dependences of the metallic and insulating regimes are shown in Fig. 10; for the metallic regime, $\sigma(\omega)\propto\omega^{1/2}$, in contrast to the ω^2 dependence of the insulating regime for $\omega_c<600$ cm^{-1}.

The corresponding $\varepsilon_1(\omega)_{\text{LD}}$ for the localization-modified Drude model can be obtained through the KK transformation of $\varepsilon_2(\omega)_{\text{LD}}=4\pi\sigma_{\text{LD}}(\omega)/\omega$ given as

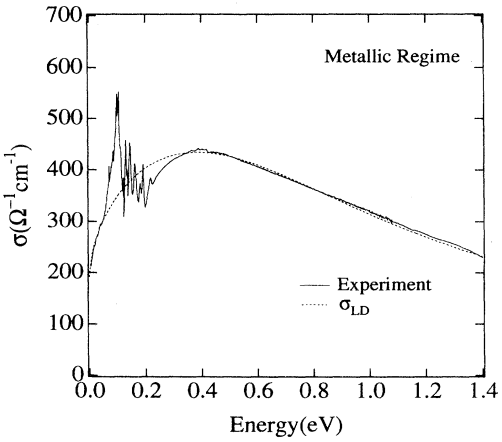

FIG. 9. Comparison of the measured $\sigma(\omega)$ (solid line) of $PPy(PF_6)$ in the metallic regime at 300 K with that calculated (dotted line) from the localization-modified Drude model as described by Eq. (3), with the following parameters: $\omega_p = 14\,200$ cm^{-1} (1.8 eV), $1/\tau = 9600$ cm^{-1} (1.2 eV), and $k_F l = 1.6$.

$$\varepsilon_1(\omega)_{LD} = \varepsilon_\infty + \left[\frac{2}{\pi}\right] P\int_0^\infty \frac{\omega'\varepsilon_2(\omega')_{LD}}{(\omega')^2-\omega^2} d\omega' , \quad (4)$$

where P denotes the principal part of the integral. Figure 11 shows that the calculated $\varepsilon_1(\omega)_{LD}$ is in excellent agreement with the measured $\varepsilon_1(\omega)$ with $\varepsilon_\infty \approx 1.1$. As evident in the calculated $\varepsilon_1(\omega)_{LD}$, the increase of $\varepsilon_1(\omega)$ as $\omega \to 0$ for $\hbar\omega < 0.2$ eV is associated with the weak-localization effect corresponding to the suppression of $\sigma_{LD}(\omega)$ at low frequencies. The calculated $\varepsilon_1(\omega)_{LD}$ predicts a rapid increase in $\varepsilon_1(\omega)$ as $\omega \to 0$ in the extrapolated region ($\omega < 20$ cm^{-1}), implying a divergence in ε_1 as $\omega \to 0$. This divergence is associated with the dielectric catastrophe, a signature of the M-I transition.[2,31–34] This phenomena has been observed in the critical regime near the M-I transition in Si:P.[35] In such a system, the dielectric constant becomes very large (due to anomalous diffusion near E_C) as the M-I transition is approached, and shows a divergence at the M-I transition boundary. Indeed, this has been predicted by theory,[32]

$$\varepsilon_1 = \varepsilon_\infty + 4\pi e^2 N(E_F) L_C^2 , \quad (5)$$

for a system near the M-I transition, where L_C is the correlation length. Since both theory[2–4] and experiments[18] confirm the divergence of L_C at the M-I transition, the corresponding divergence in $\varepsilon_1(\omega)$ is expected as $\omega \to 0$.

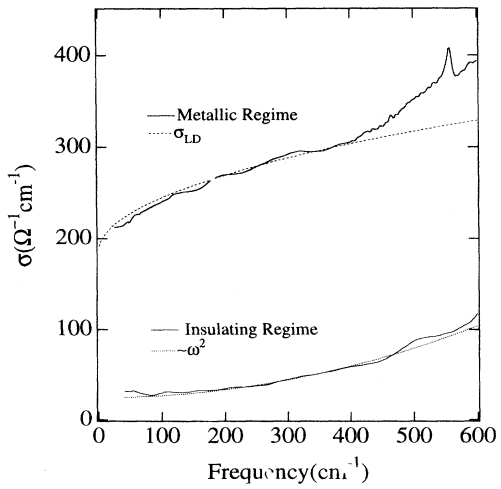

FIG. 10. Comparison of the measured $\sigma(\omega)$ (solid line) of $PPy(PF_6)$ with theoretical predictions (in the far-IR below 600 cm^{-1}) for both the metallic and insulating regimes as described in text.

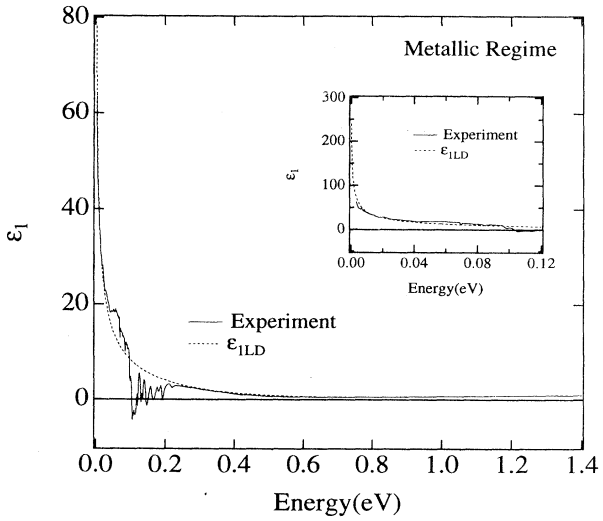

FIG. 11. Comparison of the measured $\varepsilon_1(\omega)$ (solid line) of $PPy(PF_6)$ in the metallic regime with the theoretical prediction of the localization-modified Drude model (dotted line) obtained from the KK transformation of the $\sigma_{LD}(\omega)$, as given by Eq. (4). The inset shows the low-energy part on an expanded scale.

Figure 12 compares the experimental $R(\omega)$ for the metallic regime with the calculated $R(\omega)$ obtained from $\sigma_{LD}(\omega)$ and $\varepsilon_1(\omega)_{LD}$ using the reflectance equation:

$$R(\omega) = \frac{1+|\varepsilon|-[2(\varepsilon_1+|\varepsilon|)]^{1/2}}{1+|\varepsilon|+[2(\varepsilon_1+|\varepsilon|)]^{1/2}} . \quad (6)$$

There is excellent agreement between the two curves over the entire intraband frequency range, clearly confirming the validity of the localization-modified Drude model for describing the IR optical properties of $PPy(PF_6)$ in the metallic regime. Moreover, internal consistency between the calculated optical constants involved in this analysis is implied.

The analysis of the data obtained from samples on the metallic side of the metal-insulator transition can be compared with results published earlier.[36] Although reflectance is similar, Kohlman *et al.*[36] characterize their data is in agreement with Drude metallic response, simi-

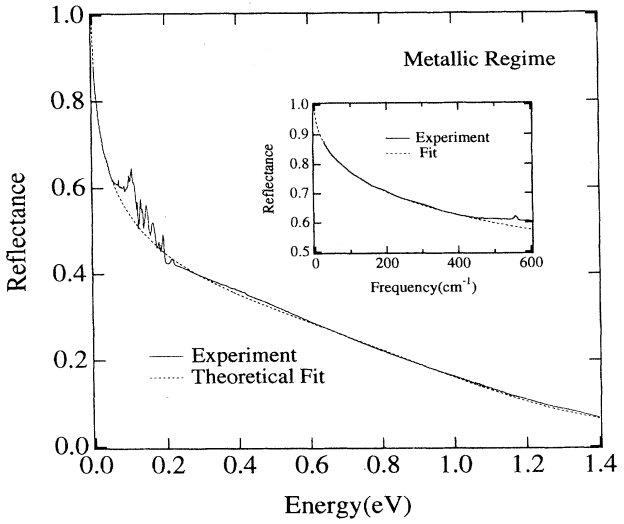

FIG. 12. The measured reflectance spectrum (solid line) of PPy(PF_6) in the metallic regime is compared with that calculated (dotted line) by the localization-modified Drude model, using Eq. (6) with $\sigma(\omega)_{LD}$ and $\varepsilon_1(\omega)_{LD}$.

lar to the behavior of usual metals. As shown in Figs. 9 and 11, we find that one must include the effects of localization in order to properly account for the details of the reflectance. Although we find $\varepsilon_1(\omega)>0$ for all frequencies at room temperatures (see Fig. 11), a crossover to $\varepsilon_1(\omega)<0$ in the far infrared is observed at lower temperatures,[37] qualitatively similar to the results reported by Kohlman *et al.* at room temperature. These differences might arise from minor differences in sample quality. Again, however, the low-temperature data are not Drude-like;[37] the results indicate that PPy(PF_6) is a disordered metal in which a gap opens for temperatures below 100 K.

F. Charge dynamics of PPy(PF_6) in the metallic regime

Analysis by the localization-modified Drude model provides information on the charge dynamics of the free carriers in the conduction band. The parameters obtained from the curve fitting are reasonable and in good agreement with other experimental results The screened plasma frequency $\Omega_p=\omega_p/(\varepsilon_\infty)^{1/2}\approx 1.7$ eV is in good agreement with the observed reflectance minimum around 1.8 eV. As we expect from the extremely broad $\sigma(\omega)$, the large scattering rate ($1/\tau=1.2$ eV) leads to $\omega_p\tau\approx 1.5$. Such a small value of $\omega_p\tau$ indicates overdamping of the plasma resonance, resulting in $\varepsilon_1(\omega)>0$ over the entire intraband energy range.

The optical mass is calculated to be $m^*=1.7m_e$ from the relation $\omega_p=(4\pi ne^2/m^*)^{1/2}$. Here the carrier concentration was assumed to be $n\approx 3.8\times 10^{21}$ cm^{-3}, i.e., one carrier per unit cell (four pyrroles).[22] This value is in excellent agreement with that obtained from the $N_{\rm eff}(\omega)$ analysis. Indeed, this consistency is expected because of the oscillator strength sum rule existing between the integrated intraband oscillator strength $N_{\rm eff}(\omega)$ and ω_p.[19]

The localization-modified Drude model yields an estimate of the dc conductivity, given as the $\omega=0$ limit of Eq. (3):

$$\sigma_{LD}(0)=\sigma_{\rm Drude}\left[1-\frac{C}{(k_Fl)^2}\right], \tag{7}$$

with $\sigma_{\rm Drude}(0)=(1/4\pi)\omega_p^2\tau$, so that one finds $\sigma_{LD}(0)\approx 200$ S/cm, in good agreement with the experimentally observed $\sigma(\omega\rightarrow 0)$. This value is slightly higher than Mott's minimum metallic conductivity $\sigma_{\rm min}=0.03e^2/\hbar a=70$ S/cm, assuming that the microscopic length scale of this system is given as an average of unit cell spacing, $a\sim 10$ Å. Note, however, that $\sigma_{\rm min}>\sigma(\omega\rightarrow 0)\approx 30$ S/cm for the insulating regime. On the other hand, in the metallic regime, $\sigma_{LD}(0)$ is slightly lower than the measured σ_{dc} at room temperature, σ_{dc} (300 K)=340 S/cm. This difference arises from the phonon-assisted hopping contribution to the dc transport measurements, whereas for the optical measurements in the IR range ($\hbar\omega>kT$) the phonon-assisted hopping does not contribute. This is supported by the contrasting temperature dependences of the σ_{dc} and $\sigma(\omega\rightarrow 0)$ in this system; σ_{dc} decreases as T is lowered,[13] while $\sigma(\omega)$ *increases* as T is lowered (at low frequencies, $\hbar\omega<0.2$ eV), reflecting metallic behavior in the far IR.[37] In this sense, $\sigma(\omega)$ gives one insight into more intrinsic metallic properties.

In studies of localization, k_Fl is an important parameter which characterizes the extent of disorder, often considered as an order parameter for disordered systems.[2–4] One of the advantages of an analysis using the localization-modified Drude model lies in the direct assessment of k_Fl. The $k_Fl\approx 1.6$ obtained from the curve-fitting procedure clearly indicates that PPy(PF_6) is not a good metal. This parameter yields an estimation for the mean free path $l\approx 10$ Å, comparable to the repeat unit along the polymer chain. Such a short mean free path confirms once again the breakdown of the normal Drude model for describing PPy(PF_6).

IV. CONCLUSION

We have investigated the reflectance spectra of PPy(PF_6) near the *M-I* transition. In particular, the spectra on the metallic and insulating sides were compared, revealing the influence of disorder on this system. The reflectance data indicate delocalized electronic states near E_F for the metallic regime and localized electronic states near E_F for the insulating regime, implying a crossover in the relative positions of E_F and the mobility edge. Thus, on the metallic side of the *M-I* transition, PPy(PF_6) is a disordered metal, while on the insulating side PPy(PF_6) is characterized as a Fermi glass. In the insulating regime, we find the following.

(i) The electronic states in the conduction band near E_F are localized, as shown in the suppression of $\sigma(\omega)$ and the increase of $\varepsilon_1(\omega)$ as $\omega\rightarrow 0$ for $\hbar\omega<0.4$ eV.

(ii) The interband transitions (2.7- and 3.7-eV features)

are broadened and weakened as a consequence of smearing of joint density of states due to disorder.

(iii) The free-carrier plasma oscillation in the conduction band is overdamped, as is evident from the positive $\varepsilon_1(\omega)$ over the intraband energy range and from the broad maximum in $\mathrm{Im}[-1/\varepsilon(\omega)]$ corresponding to $\omega_p\tau \sim 1$.

The improved sample quality obtained from the low-temperature synthesis allows a quantitative analysis of the charge dynamics involved in the conduction band, leading to the observation of the intrinsic metallic properties of $PPy(PF_6)$.

ACKNOWLEDGMENTS

We thank E. L. Yuh for experimental assistance on the far-IR measurements, and Dr. N. S. Sariciftci for providing the magnetic properties data. This work was supported by the Office of Naval Research, Kenneth Wynne, Program Officer under N00014-91-J-1235.

[1]N. W. Ashcroft and N. D. Mermin, *Solid State Physics* (Holt, Rinehart & Winston, New York, 1976).

[2]N. F. Mott, *Metal-Insulator Transitions* (Taylor & Francis, New York, 1990); N. F. Mott and M. Kaveh, Adv. Phys. **34**, 329 (1985).

[3]N. F. Mott and E. Davis, *Electronic Processes in Non-Crystalline Materials* (Clarendon, Oxford, 1979).

[4]P. A. Lee and T. V. Ramakrishnan, Rev. Mod. Phys. **57**, 287 (1985).

[5]A. J. Heeger, S. A. Kivelson, J. R. Schrieffer, and W. P. Su, Rev. Mod. Phys. **60**, 781 (1988).

[6]*Handbook of Conducting Polymers,* edited by T. A. Skotheim (Marcel Dekker, New York, 1986), Vol. 2, and references therein.

[7]J. Tsukamoto, Adv. Phys. **41**, 509 (1992).

[8]A. J. Epstein, J. M. Ginder, F. Zuo, H. S. Woo, D. B. Tanner, A. F. Richter, M. Angeloupolos, W. S. Huang and A. G. MacDiarmid, Synth. Met. **21**, 63 (1987); A. J. Epstein, J. M. Ginder, F. Zuo, R. W. Bigelow, H. S. Woo, D. B. Tanner, A. F. Richter, W. S. Huang, and A. G. MacDiarmid, *ibid.* **18**, 303 (1987); J. M. Ginder, A. F. Richter, A. G. MacDiarmid, and A. J. Epstein, Solid State Commun. **63**, 97 (1987).

[9]K. Sato, M. Yamaura, T. Hagiwara, K. Murata, and M. Tokumoto, Synth. Met. **40**, 35 (1991).

[10]T. Ishiguro *et al.*, Phys. Rev. Lett. **69**, 660 (1992).

[11]Y. Cao, P. Smith, and A. J. Heeger, Synth. Met. **48**, 91 (1992).

[12]M. Reghu, Y. Cao, D. Moses, and A. J. Heeger, Phys. Rev. B **47**, 1758 (1993); M. Reghu, C. O. Yoon, D. Moses, A. J. Heeger, and Y. Cao, *ibid.* **47**, 17 685 (1993).

[13]C. O. Yoon, M. Reghu, D. Moses, and A. J. Heeger, Phys. Rev. B **49**, 10 851 (1994); M. Reghu, C. O. Yoon, D. Moses, and A. J. Heeger, Synth. Met. **64**, 53 (1994).

[14]Z. H. Wang, E. M. Scherr, A. G. MacDiarmid and A. J. Epstein, Phys. Rev. B **45**, 4190 (1992); Z. H. Wang, A. J. Epstein, A. Ray, and A. G. MacDiramid, Synth. Met. **41-43**, 749 (1991); Z. H. Wang, C. Li, E. M. Scherr, A. G. MacDiarmid, and A. J. Epstein, Phys. Rev. Lett. **66**, 1745 (1991).

[15]M. Reghu, C. O. Yoon, Y. Cao, D. Moses, and A. J. Heeger, Phys. Rev. B **48**, 17 685 (1993).

[16]M. Reghu, C. O. Yoon, C. Y. Yang, D. Moses, Paul Smith, A. J. Heeger, and Y. Cao, Phys. Rev. B **50**, 13 931 (1994).

[17]M. Pollak and C. J. Adkins, Philos. Mag. B **65**, 855 (1992).

[18]See, for example, G. A. Thomas, M. Paalanen, and T. F. Rosenbaum, Phys. Rev. B **27**, 3847 (1983); T. G. Castner, W. N. Shafarman, and D. Koon, Philos. Mag. B **56**, 805 (1987).

[19]See, e.g., F. Wooten, *Optical Properties of Solids* (Academic, New York, 1972).

[20]M. Yamaura, K. Sato, T. Hagiwara, and K. Iwata, Synth. Met. **48**, 337 (1992); M. Yamaura, T. Hagiwara, M. Hirasaka, T. Demura, *ibid.* **28**, C157 (1989).

[21]T. Hagiwara, M. Hirasaka, K. Sato, and M. Yamaura, Synth. Met. **36**, 241 (1990).

[22]Y. Nogami, J.-P. Pouget, and T. Ishiguro, Synth. Met. **62**, 257 (1994).

[23]H. Ehrenreich and H. R. Phillip, Phys. Rev. **128**, 1622 (1962).

[24]Kwanghee Lee, A. J. Heeger, and Y. Cao, Phys. Rev. B **48**, 14 884 (1993); Synth. Met **72**, 25 (1995).

[25]X. Q. Yang, D. B. Tanner, M. J. Rice, H. W. Gibson, A. Feldblum, and A. J. Epstein, Solid State Commun. **62**, 335 (1987); Mol. Cryst. Liq. Cryst. **117**, 267 (1985).

[26]Y. H. Kim and A. J. Heeger, Phys. Rev. B **40**, 8393 (1989).

[27]K. Kim, R. H. Mckenzie, and J. W. Wilkins, Phys. Rev. Lett. **71**, 4015 (1993).

[28]Z. Ovadyahu, Phys. Rev. B **47**, 6161 (1993); Z. Ovadyahu, Physica A **200**, 462 (1993).

[29]See, e.g., *Optical Properties of Solid,* edited by F. Abeles (North-Holland, London, 1972).

[30]N. S. Sariciftci (private communication).

[31]T. G. Castner, in *Hopping Transport in Solids,* edited by M. Pollak and B. I. Shklovskii (North-Holland, Amsterdam, 1990).

[32]T. G. Castner and R. J. Deli, in *Disordered Semiconductors* (Plenum, New York, 1987).

[33]E. M. Gershenzon, A. P. Mel'nikov, and R. I. Rabinovich, in *Electron-Electron Interactions in Disordered Systems,* edited by A. L. Efros and M. Pollak (North-Holland, Amsterdam, 1985).

[34]N. F. Mott, in *Localization and Interaction in Disordered Metals and Doped Semiconductors,* edited by D. M. Finlayson, Proceedings of the 34th Scottish Universities Summer School Physics of 1986 (Scottish Universities Summer School in Physics, Saint Andrews, UK, 1986); and in *Localization 1990,* edited by K. A. Benedict and J. T. Chalker, IOP Conf. Proc. No. 108 (Institute of Physics, Bristol, 1990).

[35]G. A. Thomas, Physica B **117**, 81 (1993); M. A. Paalanen, T. F. Rosenbaum, G. A. Thomas, and R. N. Bhatt, Phys. Rev. Lett. **48**, 1284 (1982).

[36]R. S. Kohlman, J. Joo, Y. Z. Wang, J. P. Pouget, H. Koneke, T. Ishiguro, and A. J. Epstein, Phys. Rev. Lett. **74**, 773 (1995).

[37]Kwanghee Lee, Reghu M., E. L. Yuh, N. S. Sacriciftci, and A. J. Heeger, Synth. Met. **68**, 287 (1995).